

To be submitted to ApJ

A Search for Giant Pulses from Millisecond Pulsars

H. S. Knight¹ M. Bailes

Centre for Astrophysics & Supercomputing, Swinburne University of Technology, P.O. Box 218, Hawthorn VIC 3122, Australia

R. N. Manchester

Australia Telescope National Facility, CSIRO, P.O. Box 76, Epping NSW 1710, Australia

and

S. M. Ord

Centre for Astrophysics & Supercomputing, Swinburne University of Technology, P.O. Box 218, Hawthorn VIC 3122, Australia

`hknights@astro.swin.edu.au`

ABSTRACT

We have searched for microsecond-timescale broadband emission from a sample of eighteen millisecond pulsars. Our study places strong limits on such emission from several millisecond pulsars and shows that it is only present in a small subset of millisecond pulsars. Giant pulses of up to 64 times the mean pulse energy were detected from PSR J1823–3021A in the globular cluster NGC 6624. In contrast to the giant pulses of PSR B1937+21, nearly all of the giant pulses from PSR J1823–3021A were distributed within the trailing half of the main-pulse component of the integrated pulse profile. The fact that no giant pulses were observed on the leading side of the main-pulse component suggests that giant pulses are preferentially emitted closer to the last open field line than ordinary emission. The correlation between giant pulse emissivity and spin-down luminosity in millisecond pulsars suggests that the high period derivative of PSR J1823–3021A is intrinsic and is not just an artifact of its acceleration in the gravitational potential of NGC 6624.

Subject headings: pulsars:general — pulsars:individual(PSR J1823–3021A)

¹Affiliated with the Australia Telescope National Facility, CSIRO

1. Introduction

The detection of strong bursts of radio emission emanating from the Crab supernova remnant yielded the dramatic discovery of a central neutron star in the form of the Crab pulsar (Staelin & Reifenstein 1968). These giant pulses appear to be a distinct phenomenon to ordinary pulsed emission – they exhibit a variable spectral index consistent with or flatter than the integrated profile (Sallmen et al. 1999), and a pulse energy distribution showing a long high-energy tail with a power-law dependence on energy (Lundgren et al. 1995). The giant pulses are an intrinsically short timescale phenomena with individual sub-pulses having durations as brief as two nanoseconds (Hankins et al. 2003). Such “nanopulses” exhibit brightness temperatures as high as 10^{37} K.

Cognard et al. (1996) discovered giant pulses from a pulsar with substantially different characteristics to the Crab pulsar. Whilst the Crab pulsar is just 950 years old, PSR B1937+21 has a characteristic age of 237 million years and spins over 20 times faster². The Crab pulsar’s inferred surface dipole magnetic field is 10^4 times greater than that of PSR B1937+21. Cognard et al. pointed out that the two pulsars do however have the highest inferred magnetic fields at their light cylinders (B_{LC}) of all Galactic pulsars. Discoveries of giant pulses from the high B_{LC} pulsars J1824–2452 (Romani & Johnston 2001) (hereafter RJ01) and B0540–69 (Johnston & Romani 2003) have further reinforced the notion that $B_{LC} \propto P^{-2.5} \dot{P}^{0.5}$ is an indicator of giant pulse emissivity. Despite the similarity in B_{LC} , Kinkhabwala & Thorsett (2000) showed that the giant pulse emission from PSR B1937+21 exhibits important differences to that of the Crab pulsar. The giant pulses from PSR B1937+21 are not coincident with the peak of the integrated emission envelope, but instead are found in narrow $\sim 1^\circ$ phase windows on the extreme outer trailing edge of each of the main and inter-pulse regions. Interestingly, the pulsed X-ray flux from PSR B1937+21 is coincident with the giant pulse emission window rather than that of the ordinary emission (Cusumano et al. 2003; Nicastro et al. 2004).

Few strong limits on giant pulse emission from millisecond pulsars have been made due to lack of instrumentation capable of searching data at high time resolution. Edwards & Stappers (2003) and RJ01 searched for giant pulse emission from 5 and 11 millisecond pulsars respectively. Edwards & Stappers showed giant pulse emission is not manifest in the millisecond pulsar population as a whole. However, it remains unclear how many millisecond pulsars emit giant pulses of durations much shorter than the sampling intervals of these studies. In this study we obtain data on a large sample of bright millisecond pulsars using a

²Pulsar parameters in this paper were obtained using the ATNF Pulsar Catalogue (<http://www.atnf.csiro.au/research/pulsar/psrcat>)

baseband recorder system. By implementing the coherent dedispersion technique of Hankins & Rickett (1975) we can remove dispersive smearing to the nominal dispersion measure (DM) of the pulsar and obtain effective sampling times $\sim 20\text{--}70$ times shorter than Edwards & Stappers and RJ01. Here we report new limits on giant pulse emission from several high B_{LC} pulsars, and investigate a previously unknown population of giant pulses from PSR J1823–3021A.

2. Observations and Data Analysis

Observations were taken using the Parkes 64-m radio telescope on 2004 February 1–4 and June 3–6. Three observing bands centered at 685, 1341, and 1405 MHz were used. Receivers used were the 10/50 cm coaxial receiver for the 685 MHz observations and the H-OH receiver for the 1341 and 1405 MHz observations. These receivers have system equivalent flux densities on cold sky of approximately 66 and 36 Jy respectively. All data were acquired and reduced using the CPSR2 baseband recorder (Bailes 2003). This backend was used to 2-bit sample at the Nyquist rate one or two dual-polarization 64 MHz bands. The digitized data were subsequently distributed about an associated cluster of 28 dual-processor 2.2 GHz Xeon computers. Software then formed a coherent filterbank of 256 channels dedispersed to the nominal DM of the pulsar in a similar fashion to that detailed by van Straten (2003). After detection the synthetic filterbank data were written to disk and total intensity pulse profiles were formed by folding at the topocentric pulse period.

Data were searched at time resolutions in the range 4–128 μs for dispersed emission spikes. Data segments of duration 16.7 s containing consecutive samples totaling 11σ above the local mean were reduced in greater detail to produce plots of giant pulse candidates. The remaining data and their associated raw baseband files that did not meet this criteria were deleted to free sufficient disk space for further observations.

We applied our technique to short observations of PSR B1937+21 and PSR J1824–2452 (PSR B1821–24) and quickly found giant pulses. Subsequently we observed a sample of 18 millisecond pulsars, as summarized in Table 1. Names and distinguishing parameters of the pulsars (period, period derivative, spin-down luminosity, and magnetic field at the light cylinder) are shown in columns 1–5, the observation frequency is shown in column 6, while the time and number of pulses observed are shown in columns 7–8. Columns 9 and 10 show the mean pulse energy observed and the detection energy threshold for emission lasting $\lesssim 4\mu\text{s}$. The effective energy threshold is higher for pulses that are broader than $4\mu\text{s}$.

3. Results

3.1. PSR J1603–7202

Observations of the binary millisecond pulsar J1603–7202 revealed 497 large-amplitude broadband spike detections. The sample of pulse events found were typically resolved to durations of 8–300 μ s. This is in stark contrast to our observations of giant pulses from PSR B1937+21 and PSR J1824–2452, where almost all giant pulses were unresolved at the initial 4 μ s sampling time. Many of the pulses from PSR J1603–7202 had significant substructure across a wide phase range. Although the pulses had very high peak flux densities, their energies were typically only a few times the average pulse energy. The large pulse detection count is a result of our energy threshold being just 0.2 $\langle E \rangle$ at 4 μ s. The emission events from PSR J1603–7202 are therefore best interpreted as microstructure and are not further discussed in this paper.

3.2. PSR J1823–3021A

PSR J1823–3021A is an enigmatic 5.4-ms pulsar that has the lowest characteristic age, $\tau_{\text{char}} = P/(2\dot{P}) = 25$ Myr, of all known millisecond pulsars. Its inferred spin-down energy loss rate ($\dot{E} \propto P^{-3}\dot{P}$) is the third highest of all millisecond pulsars after PSR B1937+21 and PSR J1824–2452. However, PSR J1823–3021A lies less than 1" from the centre of the dense globular cluster NGC 6624 (Sosin & King 1995; Hobbs et al. 2004) and therefore acceleration in the cluster potential undoubtedly contributes to the observed \dot{P} (see e.g. Stappers 1997).

In the 685, 1341, and 1405 MHz bands respectively, we detected 5, 7, and 14 large-amplitude broadband emission events. The signal to noise ratios of the events were optimal at the DM of PSR J1823–3021A. All but one of the large-amplitude pulses were clustered around a small phase window approximately 0.03 periods wide on the trailing half of the dominant pulse component of PSR J1823–3021A (See Fig. 1). The sole significant pulse found outside this phase window was coincident with the earlier half of the small leading component of PSR J1823–3021A. The detection of this pulse at 685 MHz where only 5 of the 26 detections were made suggests the giant pulse spectral index is steep within this window. As all giant pulses found are related in phase to emission from PSR J1823–3021A we conclude PSR J1823–3021A is the source of the emission and not any other cluster source.

Data not flagged as potentially containing a giant pulse were deleted online. Consequently only a few minutes of data were available post-observation to determine the pulse

energy distribution. Each of the remaining 685, 1341, and 1405 MHz datasets was re-folded to produce single-pulse profiles of 128, 256, and 256 bins respectively. By assuming each giant pulse to be just a single bin wide and obtaining the peak flux for several phase windows the cumulative probability distribution of pulse energy was determined. The 685 MHz distribution is shown in Fig. 2. As the sample of pulses still available is biased, the probabilities of the giant pulses that had already been identified were shifted to take into account all data taken. At each frequency the pulses occurring on the second half of the main pulse exhibit a clear power-law tail of giant pulses. Fitting for the cumulative energy distribution yielded power-law exponents of approximately -2 for the 685-MHz data and -3 for the data at the two higher frequencies. While these indices appear different, they are based on a small number of events; further observations are required to verify any frequency dependence of the power-law slope.

The mean FWHM of the giant pulses was $21\,\mu\text{s}$ for the 685 MHz pulses, and $7\,\mu\text{s}$ for the higher frequencies. Visual inspection of the stronger pulses at 685 MHz suggests that they are broadened by interstellar scattering. We attribute the greater detection counts at 1341 and 1405 MHz to their narrower pulse widths. Future giant pulse searches have the potential to be more productive at high frequencies where scattering and dispersion will not dampen peak pulse fluxes as markedly. The dampening effect of pulse broadening can readily be demonstrated by looking at the peak fluxes of the largest pulses. At 685 and 1405 MHz the largest pulses peaked at 45 and 20 Jy, or around 680 and 1700 times the mean peak flux respectively. The brightest pulse at 1405 MHz would have a peak flux density of 8 kJy at 1 kpc if it could be resolved to $1\,\mu\text{s}$, which is less than the corresponding values found for PSRs J1824–2452 (30 kJy) and B1937+21 (20 kJy) (Johnston & Romani 2003). When viewed in terms of the average pulse energy the brightest pulses from PSR J1823–3021A in each band had comparable energies (See Fig. 1). The most energetic pulse was $64\langle E \rangle$ at 685 MHz. At 1405 MHz, 6 pulses were greater than 28 times the mean pulse energy, yielding $P(E > 28\langle E \rangle) \sim 4.6 \times 10^{-6}$. In comparison, RJ01 measure for PSR J1824–2452 at 1517.75 MHz $P(E > 28\langle E \rangle) \sim 8.5 \times 10^{-7}$, which is around twice the value for PSR B1937+21.

3.3. Limits for other Pulsars

No large-amplitude emission events were detected for the remaining 16 millisecond pulsars. Only PSRs J0034–0534, J1843–1113, and B1957+20 had integrated flux densities lower than PSR J1823–3021A at frequencies above 1300 MHz. The null result for the majority of the sources shows that giant pulse emission is not prevalent amongst millisecond pulsars. Of particular note were the lack of giant pulses from the short-period and high

B_{LC} pulsars J1843–1113 and B1957+20. Joshi et al. (2004) report the detection from PSR B1957+20 of a single large-amplitude pulse ($\sim 129\langle E \rangle$) and 5 marginal candidates in a sample of 10^6 pulses taken at 610 MHz. It is difficult to understand why Joshi et al. were able to detect large-amplitude emission and we were not. For PSR B1957+20 the central 48-MHz of our band at 685 MHz gave approximately 1.2 times the sensitivity of the 16-MHz system of Joshi et al. for an equal sampling interval. Furthermore, we observed nearly five times as many pulses from PSR B1957+20 with an effective sampling rate that was over 64 times faster. One possible explanation is that PSR B1957+20 emits strong giant pulses at a very low frequency and Joshi et al. were fortunate enough to chance upon such an event, whilst we were not. Another explanation is that the solitary pulse of Joshi et al. is spurious. Our observations indicate that PSR B1957+20 should not currently be classed as a millisecond pulsar which emits frequent or strong giant pulses.

4. Discussion

The giant pulses from PSR J1823–3021A differ from those of PSR B1937+21 in that they are not clustered around the extreme trailing edge of the pulse components. Such a difference is probably due to viewing geometry rather than a different emission mechanism, and so a geometric interpretation can be conjectured. The two pulse components of PSR B1937+21 are separated in phase by nearly 180° and therefore the pulsar has been interpreted as an orthogonal rotator (Stairs et al. 1999). With each pulse component having an associated giant pulse emission region it is natural then to assume that both poles are endowed with the conditions necessary for giant pulse emission. Rather than interpreting the two pulse components of PSR J1823–3021A as emission from opposing poles, we suggest that they represent two cuts of a cone of emission that lies close to the last open field line. The giant pulses appear to be preferentially emitted towards the outside edge of this emission cone compared to the ordinary emission. In addition, the giant pulses may originate higher in the magnetosphere than ordinary emission. Of course, with only one giant pulse detected on the leading component of PSR J1823–3021A more data needs to be taken to clarify such speculation. PSR B1937+21 is then interpreted as having narrow giant pulse envelopes much closer to the last open field line than its ordinary emission envelopes.

With around $\sim 70\%$ of millisecond pulsars found in binary systems it is interesting to note that the three millisecond pulsars now known to emit giant pulses are all solitary. Along with PSR J0737–3039A and the solitary globular cluster pulsar J1910–5959D the three millisecond pulsars in question have the lowest characteristic ages of all millisecond pulsars. If they were spun-up through accretion from a binary companion (see e.g. Bhattacharya &

van den Heuvel 1991) they must have ablated or lost their companions in their short lifetimes. If pulsars can ablate a binary companion in just a few million years it is not surprising that it is the energetic giant-pulse emitters that are solitary. Observations of solitary millisecond pulsars in globular clusters could therefore yield further detections of giant pulse emission.

Giant pulses of energy $\gtrsim 28\langle E \rangle$ emanating from PSR J1823–3021A were found at a higher rate than for PSR B1937+21 and PSR J1824–2452. The rate at 1341 and 1405 MHz is sufficiently high that if the pulsar were twice as weak our observations would only have been detected it through giant pulses. Despite the high rate of giant pulse activity from PSR J1823–3021A we failed to detect any giant pulse activity from other pulsars with similar or higher inferred B_{LC} such as PSR B1957+20. Radiation from PSR B1957+20 ablates gas from its companion (Fruchter et al. 1990). Our non-detection of giant pulses from PSR B1957+20 may result from the ablated gas causing excess scattering on microsecond timescales. Other systems like PSR J1843–1113 and PSR J0034–0534 may not emit enough strong giant pulses for us to detect or simply not emit giant pulses at all.

Acceleration of PSR J1823–3021A in the potential of NGC 6624 could also mean that its intrinsic spin-down rate and B_{LC} are greater than the values inferred from observation. Bailes et al. (2004) have shown that PSR J1823–3021A exhibits cubic timing residuals and has a spin-frequency second derivative $\ddot{\nu} = 6.1 \times 10^{-25} \text{ s}^{-3}$. The magnitude of $\ddot{\nu}$ is consistent with the empirical relation for timing noise found by Arzoumanian et al. (1994). Such timing noise is supportive of the suggestion that the pulsar’s intrinsic spin-down rate is large and that it is reasonably youthful. However, explaining the high giant pulse emissivity of PSR J1823–3021A through a large intrinsic \dot{P} implies that the observed characteristic age is larger than the true age. Considering the average characteristic age of field millisecond pulsars is 7 Gyr, the chances of a millisecond pulsar with an age of $\lesssim 25$ Myr being amongst the ~ 100 known seem low. Two unrecycled pulsars are also found in NGC 6624 (Biggs et al. 1994; Chandler 2003). If PSR J1823–3021A does have a low age then the existence of these short-lived slow pulsars implies NGC 6624 could have a large pulsar formation rate in the current epoch. Further evidence favouring a low age for PSR J1823–3021A could be made by observations of microglitches similar to those observed in PSR J1824–2452 (Cognard & Backer 2004).

Phenomena such as field-line current sweepback mean that the magnetic field at the light cylinder has a significantly different structure to that of the surface field. Despite this, we may conjecture that magnetic inclination angle plays a role in explaining why PSR J1823–3021A emits frequent giant pulses and why PSR B1957+20 has not been found to do so. However, Joshi et al. (2004) report that PSR J0218+4232 emits large-amplitude pulses of up to 51 times the mean pulse intensity. PSR J0218+4232 has a larger B_{LC} than PSR

J1823–3021A, but has significant unpulsed radio emission and has been interpreted as a nearly aligned rotator (Navarro et al. 1995; Stairs et al. 1999). If the large-amplitude pulses of PSR J0218+4232 are giant pulses they spoil a simple geometrical interpretation for why PSR B1957+20 does not appear to emit strong giant pulses despite its high B_{LC} .

The fact that the giant pulse emitting pulsars all have very high B_{LC} is unsurprising in many respects – it is natural to expect that those pulsars with the largest magnetic fields and fastest spin rates would exhibit energetic phenomena not found in the emission of less extreme millisecond pulsars. Perhaps then there are other contributing factors that are more important than B_{LC} ? RJ01 have suggested that a narrow X-ray pulse with a hard spectrum could be a better indicator of a magnetospheric geometry conducive to giant pulse emission. Of the millisecond pulsars observed in this study only PSR J2124–3358 has been found to pulse in the X-ray band (Becker & Trümper 1999). However, its pulse is not narrow like those of PSR B1937+21 and PSR J1824–2452 (Cusumano et al. 2003; Nicastro et al. 2004; Mineo et al. 2004). X-ray timing observations of PSR J1823–3021A could therefore help confirm whether or not the existence of a narrow X-ray pulse correlates with emission of radio giant pulses. Spin-down energy and X-ray luminosity are linearly correlated for rotation powered pulsars (Becker & Trümper 1997). Therefore it is interesting to note that PSRs B1937+21, J1824–2452, and J1823–3021A have by far the highest inferred spin-down energy loss rates of all millisecond pulsars. Perhaps then, at least for millisecond pulsars, X-ray luminosity is a proxy and \dot{E} dictates giant pulse emissivity. Information on correlations with high energy emission can be gleaned through further radio observations of PSR J0218+4232, whose X-ray and γ -ray emission properties are comparatively well known (Kuiper et al. 2000; Kuiper et al. 2002; Webb et al. 2004).

5. Conclusions

We have undertaken a survey for giant pulse emission from millisecond pulsars and detected strong microsecond-timescale giant pulses from PSR J1823–3021A. The strongest giant pulse was found at 685 MHz and had over 64 times the energy of the average pulse. The majority of giant pulses were found above 1300 MHz where scattering was not significant at our $4\mu\text{s}$ sampling time. No giant pulse emission was discovered from other pulsars with similar or higher B_{LC} to that of PSR J1823–3021A. In particular, no giant pulses were found from B1957+20. If the inferred B_{LC} is the sole determinant of giant pulse emissivity, the emission of giant pulses from PSR J1823–3021A can be explained by invoking a cluster acceleration that provides a large negative contribution to the measured \dot{P} of PSR J1823–3021A and consequently lessens the derived B_{LC} . This in turn would imply that PSR J1823–3021A

is very young, and that NGC 6624 presently has a large pulsar formation current. Alternatively, ablated gas from the companion of PSR B1957+20 might scatter-broaden any giant pulses below our detection threshold. The three millisecond pulsars that are known to emit giant pulses have the highest inferred spin-down luminosities of all millisecond pulsars, and therefore $\dot{E} \propto P^{-3}\dot{P}$ rather than $B_{LC} \propto P^{-2.5}\dot{P}^{0.5}$ may be a better indicator of giant pulse emission. Future studies of giant pulse emission at high radio frequencies will avoid complications arising from scattering-induced signal degradation, and therefore reveal the true widths and brightnesses of giant pulses and help establish the true indicators of giant pulse emissivity. X-ray timing observations of PSR J1823–3021A offer the opportunity to see whether there is a phase correlation between the giant pulse and X-ray emission envelopes. Such a correlation would add strong support to the notion that giant pulses emanate from a similar region of the pulsar magnetosphere as high energy emission.

The Parkes radio telescope is part of the Australia Telescope which is funded by the Commonwealth of Australia for operation as a National Facility managed by CSIRO. We thank A. Hotan for observing assistance, C. West for use of disks and W. van Straten for software assistance. HSK acknowledges the support of a CSIRO Postgraduate Student Research Scholarship.

REFERENCES

Arzoumanian, Z., Nice, D. J., Taylor, J. H., & Thorsett, S. E. 1994, *ApJ*, 422, 671

Bailes, M. 2003, in *Radio Pulsars*, ed. M. Bailes, D. J. Nice, & S. Thorsett (San Francisco: Astronomical Society of the Pacific), 57–64

Bailes, M., Zhu, J., & Richter, S. 2004, in *Binary Pulsars*, ed. F. Rasio & I. H. Stairs (San Francisco: Astronomical Society of the Pacific), in press

Becker, W. & Trümper, J. 1997, *A&A*, 326, 682

Becker, W. & Trümper, J. 1999, *A&A*, 341, 803

Bhattacharya, D. & van den Heuvel, E. P. J. 1991, *Phys. Rep.*, 203, 1

Biggs, J. D., Bailes, M., Lyne, A. G., Goss, W. M., & Fruchter, A. S. 1994, *MNRAS*, 267, 125

Chandler, A. M. 2003, PhD thesis, California Institute of Technology

Cognard, I. & Backer, D. C. 2004, *ApJ*, 612, L125

Cognard, I., Shrauner, J. A., Taylor, J. H., & Thorsett, S. E. 1996, *ApJ*, 457, L81

Cusumano, G., Hermsen, W., Kramer, M., Kuiper, L., Löhmer, O., Massaro, E., Mineo, T., Nicastro, L., & Stappers, B. W. 2003, *A&A*, 410, L9

Edwards, R. T. & Stappers, B. W. 2003, *A&A*, 407, 273

Fruchter, A. S., Berman, G., Bower, G., Convery, M., Goss, W. M., Hankins, T. H., Klein, J. R., Nice, D. J., Ryba, M. F., Stinebring, D. R., Taylor, J. H., Thorsett, S. E., & Weisberg, J. M. 1990, *ApJ*, 351, 642

Hankins, T. H., Kern, J. S., Weatherall, J. C., & Eilek, J. A. 2003, *Nature*, 422, 141

Hankins, T. H. & Rickett, B. J. 1975, in *Methods in Computational Physics Volume 14 — Radio Astronomy* (New York: Academic Press), 55–129

Hobbs, G., Lyne, A. G., Kramer, M., Martin, C. E., & Jordan, C. A. 2004, *MNRAS*, 353, 1311

Johnston, S. & Romani, R. W. 2003, *ApJ*, 590, L95

Joshi, B. C., Kramer, M., Lyne, A. G., McLaughlin, M. A., & Stairs, I. H. 2004, in IAU Symposium, 319

Kinkhabwala, A. & Thorsett, S. E. 2000, *ApJ*, 535, 365

Kuiper, L., Hermsen, W., Verbunt, F., Ord, S. M., Stairs, I. H., & Lyne, A. G. 2002, *ApJ*, 577, 917

Kuiper, L., Hermsen, W., Verbunt, F., Thompson, D. J., Stairs, I. H., Lyne, A. G., Strickman, M. S., & Cusumano, G. 2000, *A&A*, 359, 615

Lundgren, S. C., Cordes, J. M., Ulmer, M., Matz, S. M., Lomatch, S., Foster, R. S., & Hankins, T. 1995, *ApJ*, 453, 433

Mineo, T., Cusumano, G., Massaro, E., Becker, W., & Nicastro, L. 2004, *A&A*, 423, 1045

Navarro, J., de Bruyn, G., Frail, D., Kulkarni, S. R., & Lyne, A. G. 1995, *ApJ*, 455, L55

Nicastro, L., Cusumano, G., Löhmer, O., Kramer, M., Kuiper, L., Hermsen, W., Mineo, T., & Becker, W. 2004, *A&A*, 413, 1065

Romani, R. & Johnston, S. 2001, *ApJ*, 557, L93

Sallmen, S., Backer, D. C., Hankins, T. H., Moffett, D., & Lundgren, S. 1999, *ApJ*, 517, 460

Sosin, C. & King, I. R. 1995, *AJ*, 109, 639

Staelin, D. H. & Reifenstein, III, E. C. 1968, *Science*, 162, 1481

Stairs, I. H., Thorsett, S. E., & Camilo, F. 1999, *ApJS*, 123, 627

Stappers, B. W. 1997, PhD thesis, Australian National University

van Straten, W. 2003, PhD thesis, Swinburne University of Technology

Webb, N. A., Olive, J.-F., & Barret, D. 2004, *A&A*, 417, 181

Table 1. Pulsars searched for giant pulse emission.

PSR	P (ms)	\dot{P} (10^{-21} s/s)	\dot{E} ($\times 10^{32}$ ergs/s)	B_{LC} ($\times 10^3$ G)	ν (MHz)	t_{obs} (s)	N_p ($\times 10^5$)	$\langle E \rangle$ (Jy · μ s)	E_{lim} ($\langle E \rangle$)
J0034–0534	1.88	4.96	300	138	685 1341	2473,3251 12897	13,17 69	4.2,6.3 not detected	39,26 unknown
J0613–0200	3.06	9.57	130	56.6	1341 1405	4056,2471 3190	13,8.0 10	19,13 16	4.5,6.3 5.3
J0711–6830	5.49	14.90	36	16.4	685 1341 1405	1938 7874,2466 7968	3.5 14,4.5 15	55 21,36 36	3.0 3.9,2.3 2.3
J0737–3039A ^a	22.70	1740	59	5.10	685 1341 1405	4116 7775	1.8 3.4	310 100	0.6 0.8
J1022+1001	16.45	43.41	3.8	1.80	1341 1405	4772,4202 4951	2.9,2.5 3.0	30,290 19	2.8,0.3 4.3
J1603–7202	14.84	15.64	1.9	1.40	1341 1405	2315 2473	1.6 1.7	360 200	0.2 0.4
J1629–6902	6.00	10.0	18	10.8	685 1341 1405	3652 2675 2655	6.1 4.5 4.4	61 11 11	3.0 8.1 7.7
J1643–1224	4.62	18.49	74	28.1	1341 1405	2877 2874	6.2 6.2	39 36	2.2 2.4
J1713+0747	4.57	8.54	35	19.6	1341 1405	902 947	2.0 2.1	82 28	1.1 3.2
J1730–2304	8.12	20.21	15	7.17	1341 1405	2659 2603	3.3 3.2	51 50	1.9 1.9
J1732–5049	5.31	13.8	36	17.1	685 1341 1405	1493 3205 3204	2.8 6.0 6.0	55 16 12	4.1 5.8 7.4
J1744–1134	4.07	8.94	52	26.8	1341 1405	2919 2558	7.2 6.3	6.9 15	13 6.0
J1823–3021A	5.44	3384.14	8300 ^b	253 ^b	685 1341 1405	6136 6029 7274	11 11 13	38 5.4 6.5	5.9 17 14
J1843–1113	1.85	9.59	600	201	685 1341	3160 8971	17 48	11 2.4	25 41
J1857+0943	5.36	17.84	46	19.0	1341 1405	3360 3355	6.3 6.3	17 53	5.8 1.8
B1957+20	1.61	16.85	1600	376	685 1341	3385,4348 11009	21,27 68	16,12 not detected	12,16 unknown
J2124–3358	4.93	20.54	68	25.2	1341 1405	1575 1580	3.2 3.2	37 39	2.3 2.1
J2145–0750	16.05	29.86	2.8	1.59	1341 1405	1340 1333	0.83 0.83	50 83	1.7 1.0

^aDouble pulsar.

^bDisregards acceleration in potential of globular cluster NGC 6624.

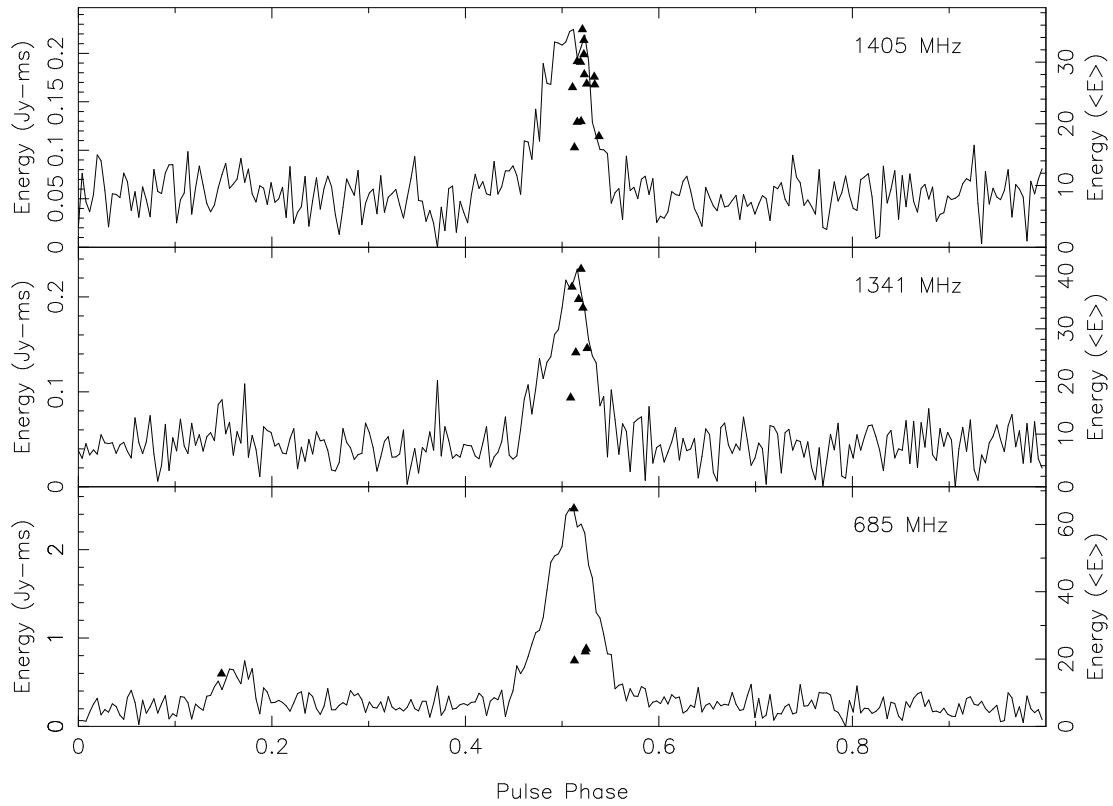


Fig. 1.— Mean pulse profiles for PSR J1823–3021A at three frequencies. The triangles show the pulse phase and energy of the detected giant pulses.

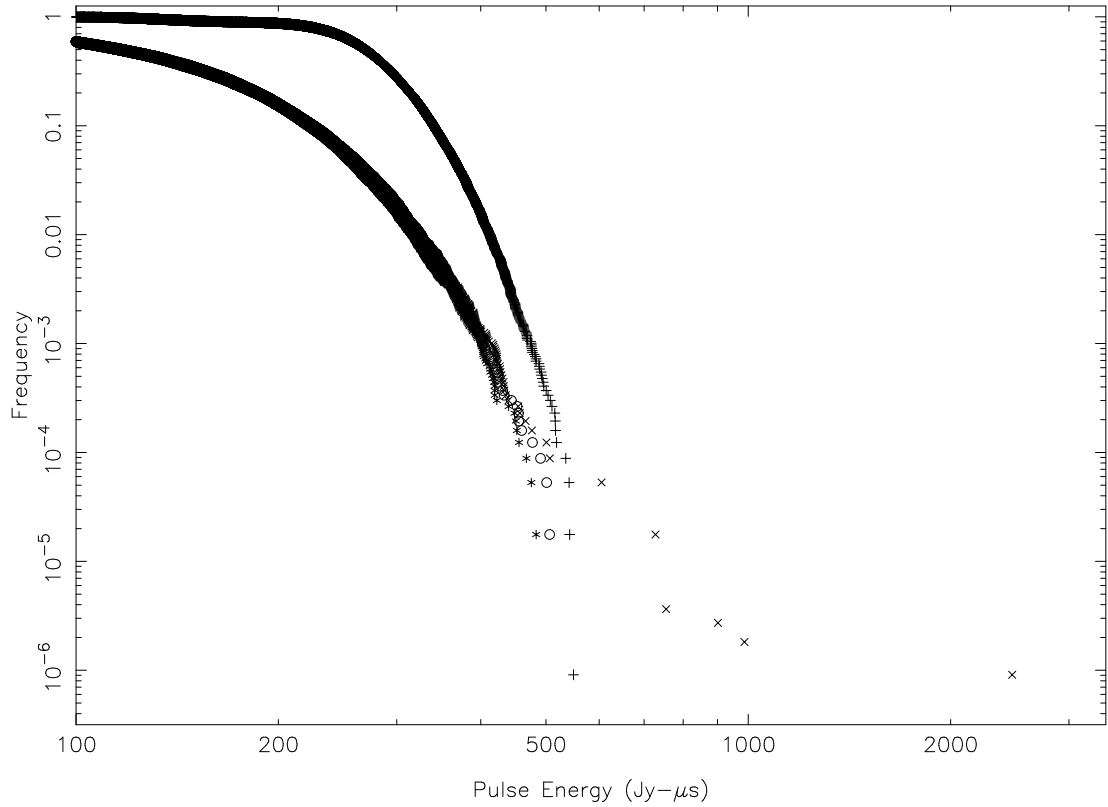


Fig. 2.— Cumulative distribution of pulse energies at 685 MHz for PSR J1823–3021A. Stars denote a phase window $[-0.04, 0]$; crosses denote $[0, 0.04]$; circles denote $[0.04, 0.08]$ where phase zero is defined as the peak of the integrated profile. Pluses denote other pulsar phases.